Loss of CHSY1, a Secreted FRINGE Enzyme, Causes Syndromic Brachydactyly in Humans via Increased NOTCH Signaling

Jing Tian,[1] Ling Ling,[1] Mohammad Shboul,[1] Hane Lee,[2] Brian O'Connor,[2] Barry Merriman,[2] Stanley F. Nelson,[2] Simon Cool,[1] Osama H. Ababneh,[3] Azmy Al-Hadidy,[3] Amira Masri,[3] Hanan Hamamy,[4] and Bruno Reversade[1,5,*]

We delineated a syndromic recessive preaxial brachydactyly with partial duplication of proximal phalanges to 16.8 Mb over 4 chromosomes. High-throughput sequencing of all 177 candidate genes detected a truncating frameshift mutation in the gene *CHSY1* encoding a chondroitin synthase with a Fringe domain. CHSY1 was secreted from patients' fibroblasts and was required for synthesis of chondroitin sulfate moieties. Noticeably, its absence triggered massive production of JAG1 and subsequent NOTCH activation, which could only be reversed with a wild-type but not a Fringe catalytically dead *CHSY1* construct. In vitro, depletion of *CHSY1* by RNAi knockdown resulted in enhanced osteogenesis in fetal osteoblasts and remarkable upregulation of *JAG2* in glioblastoma cells. In vivo, *chsy1* knockdown in zebrafish embryos partially phenocopied the human disorder; it increased NOTCH output and impaired skeletal, pectoral-fin, and retinal development. We conclude that CHSY1 is a secreted FRINGE enzyme required for adjustment of NOTCH signaling throughout human and fish embryogenesis and particularly during limb patterning.

Introduction

Precise diagnosis of brachydactylies, defined by the shortening of fingers and/or toes, is often difficult because of their vast diversity and partial clinical overlap. Five main types of brachydactylies, termed brachydactyly (BD) types A– E (MIM 112500, MIM 112600, MIM 112700, MIM 112800, MIM 112900, MIM 112910, MIM 113000, MIM 113100, MIM 113200, MIM 113300, MIM 112440, and MIM 607004), are classified according to which metacarpals and/or metatarsals, phalanges, and digits are affected.[1] At the molecular level, extracellular components of two signaling pathways, BMP/GDF and Hedgehog, have been shown to cause shortening of digits in humans. Defective BMP/GDF signaling accounts for BDA2, BDB, and BDC and can be caused by mutations in the genes encoding the extracellular BMP antagonist NOGGIN (MIM 602991), the BMP ligand GDF5 (MIM 601146), BMP2 (MIM 112261), and the BMP receptors BMPR1B (MIM 603248) and ROR2 (MIM 602337).[2–6] The Hedgehog pathway accounts for BDA1, which is caused by mutations in the ligand IHH (MIM 600726), and mutations in *SHH* (MIM 600725) cause triphalangeal thumb–polysyndactyly syndrome (MIM 174500).[7,8] Recently, mutations in the extracellular ligand PTHLH (MIM 168470) were found to be responsible for BDE, which can also be caused by HOXD13 (MIM 142989) mutations.[9,10]

Here we report on the genetic etiology of a syndromic recessive preaxial brachydactyly caused by a loss-of-function mutation in the evolutionarily conserved gene *CHSY1* (MIM 608183). *CHSY1* encodes a type II transmembrane protein comprising a Fringe motif and a glycosyltransferase domain. CHSY1 was found to be secreted, and functional experiments carried out in patients' cells, human fetal osteoblasts cells, and gliobastoma cells revealed remarkable NOTCH upregulation in the absence of CHSY1 activity. Knockdown of *chsy1* in developing zebrafish embryos was able to partially phenocopy the human disorder: it enhanced Notch signaling and impaired skeletal and pectoral-fin development while triggering dramatic retinal overgrowth. Taken together, our results identify an additional layer of control in the genetic pathway that operates in the vertebrate developing limb. Our data also suggest that CHSY1, because of its FRINGE activity, might represent another class of extracellular modulators of NOTCH signaling.

Material and Methods

Patients and Clinical Assessment

The affected children were initially diagnosed at the National Center for Diabetes, Endocrinology & Genetics in Jordan by Prof. Hanan Hamamy. Genomic DNA from saliva samples (Oragene, Canada) from the five members of this kindred and skin biopsies from one affected sibling (II:2) and his unaffected sister (II:1) were obtained after parents gave their informed consent and the local ethics commission gave its approval.

Genotyping and Homozygosity Mapping

To perform homozygosity and identity-by-descent (IBD) mapping, we analyzed the SNP chip data of the affected and unaffected siblings by using custom programs (B. Merriman) written in the Mathematica (Wofram Research) data-analysis software. In brief, we determined candidate IBD homozygous blocks in an individual

[1]Institute of Medical Biology, A*STAR, Singapore; [2]Department of Human Genetics, David Geffen School of Medicine, University of California, Los Angeles, Los Angeles, CA 90095, USA; [3]Departments of Ophthalmology, Radiology and Pediatrics, Faculty of Medicine, University of Jordan, Jordan; [4]Department of Genetic Medicine and Development, Geneva University Hospital, Geneva, Switzerland; [5]Department of Pediatrics, National University of Singapore, Singapore
*Correspondence: bruno@reversade.com
DOI 10.1016/j.ajhg.2010.11.005.

as follows: using the Illumina 610k SNP Chip (Human610-Quadv1_B) genotype data, we used AB genotypes to define boundaries of homozygous blocks. Blocks that were larger than 2 cM in size were classified as candidate IBD homozygous blocks. Centi-Morgan distances between SNPs were determined from the HapMap Phase II recombination rate map. Regions of identity (both alleles inherited IBD) between pairs of siblings were determined in a similar pedigree-free fashion. The final exclusion mapping that allowed us to obtain candidate disease loci was performed by mathematical manipulation of the various intervals defined by homozygosity and identity mapping. Specifically, we defined candidate disease loci as those that were homozygous identical by descent in affected siblings, identical by descent between affected siblings, and not identical by descent for unaffected siblings. We obtained candidate disease loci by taking the mathematical intersection of the intervals of homozygosity and identity, respectively, and then the mathematical complement of these by the intervals of identity between affected-unaffected sibling pairs.

Capture of Genomic Loci

In brief, custom arrays (Agilent 244K) were designed to target every exonic sequence of the genes present in the four homozygous indentical-by-descent regions (chr3: 147266776–155630168; chr5: 168552990–174355393; chr12: 18663–545927; and chr15: 99141618–100314150), excluding the highly repeated regions. In total, 1009 contigs encompassing 320,677 bp were targeted. DNA library for one affected subject was prepared according to the Illumina library generation protocol version 2.3 and was hybridized to the custom arrays according to the Agilent CGH 244K array protocol, then washed, eluted, and amplified. The sample was submitted to one channel of Illumina flowcell and sequenced by Illumina Genome Analyzer (GAII) according to the standard manufacturer's protocol. The image data were processed by the provided GA Pipeline (Firecrest version 1.3.4 and Bustard version 1.3.4), and all sequences were aligned to the human reference genome (UCSC build 18) by Blat-like Fast Accurate Search Tool (BFAST). We filtered mismatches to identify variants that were seen ten or more times and that did not overlap with a known dbSNP129 entry polymorphism. Non-synonymous mutations were identified with additional SeqWare tools and the "knownGene" gene model from the UCSC hg18. The open-source SeqWare project that provides a LIMS tool for tracking samples (SeqWare LIMS) and a pipeline for sequence analysis (SeqWare Pipeline) was used throughout this work.

Mutation Analysis

Positional candidate genes were obtained from the GenBank and Ensembl databases. Genes were analyzed by direct sequencing of DNA with primers flanking each exon. Primer sequences were based on the reference sequences of each gene. The primer sequences for *CHSY1* (NM_014918.4) and *HTLF* (NM_002158.3) mutation screening are given in Table S4. Sequence analysis was done with the BigDye Terminator cycle sequencing kit (Applied Biosystems, Foster City, CA), and products were run on a 3730 DNA Analyzer (Applied Biosystems, Foster City, CA).

Cell Culture

Primary human skin fibroblasts were cultivated in DMEM (Lonza) supplemented with 10% fetal calf serum (FCS) (Lonza). Human fetal osteoblast (hFOB) cells were obtained from ATCC (USA) and maintained in Ham's F12 DMEM supplemented with 10% FCS and 0.3 mg/ml G418 (Invitrogen, USA) at 33.5°C. Human gliobastoma (T98G) cells were obtained from ATCC (USA) and maintained in EMEM (ATCC) supplemented with 10% FCS. Inhibition of γ-secretase activity was carried out by incubation of cells with 2 or 5 μM of γ–secretase inhibitor X (Calbiochem, 565771) added fresh daily for 72 hr.

RNA Interference

hFOB and gliobastoma cells were seeded at 20,000 cells/cm^2 in 6-well plates and transfected via Lipofectamine 2000 (Invitrogen, USA) with two siRNAs specific for human *CHSY1* (25 pmol of each) or scrambled siRNA as a negative control. The siRNAs were purchased from QIAGEN (Germany), and their sequence is given in Table S4. For Taqman realtime PCR, cells were assayed 48 or 72 hr after transfection.

Quantitative PCR

RNA was isolated from patients' fibroblasts, T98G cells, and hFOB cells by the Trizol (Invitrogen) method. RNA (1 μg) was reverse transcribed with the Revert Aid kit (Fermentas) and random hexamers. Quantitative PCR was performed with Taqman probes (Applied Biosystems). Primers, ABI probes, assay IDs, and sequences are given in Table S4.

Statistical Analysis

Each experiment was repeated at least three times, and data were expressed as means ± SE. Differences among treatments were analyzed by a Student's t test. Significant differences were considered to be those with a p value of < 0.05.

Immunoblot Analysis

Supernatant fractions were obtained after incubation of primary skin fibroblasts in Pro293a-CDM conditioning serum-free media (BioWhittaker) for 72 hr. Cells were lysed in RIPA extraction buffer. Electrophoresis of samples in SDS polyacrylamide gels with or without DTT was followed by transfer on PVDF membranes. The following antibodies were used for probing immunoblots: mouse anti-ACTIN (Chemicon; Mab1501R), rat anti-NOTCH2 (Developmental Studies Hybridoma Bank; C651.6DbHN), goat anti-JAG1 (Santa Cruz Biotechnology; sc-6011), goat anti-HES1 (R&DSystems; AF3317), and rabbit anti-CHSY1 (Proteintech; 14420-1-AP).

Immunohistochemistry Analysis

For immunostaining, skin biopsies were fixed in 4% (weight/volume) paraformaldehyde in 1× PBS and embedded in wax, and sections of 5 μm were placed on coverslips. A mouse monoclonal antibody against Chondroitin Sulfate (Sigma; CS-56) was incubated for 1 hr in 10% normal goat serum at room temperature at a 1: 200 dilution. For visualization, an anti-mouse IgG-HRP (Dako) conjugate was applied. Images were collected with a stereomicroscope M205 FA equipped with an ICD camera from Leica.

Morpholino Oligos, RNA Injections, and Embryological Methods

Two 25 bp Morpholino (MO) antisense oligomers, CS1 and CS2, for zebrafish *chsy1* were obtained from Gene Tools; their sequences are given in Table S4. MOs were resuspended in sterile water to a concentration of 3 mM according to the manufacturer's instructions. Embryos were injected at the 1 cell stage with 1 nl consisting

of 0.2 nM CS1 and 1 nM CS2. Protocols for injections, whole-mount in situ hybridization, and alcian blue staining can be found at our laboratory's website. A ZeissAxioplan microscope equipped with a Zeiss AxioCam HRc was used for capturing images of embryos. Pictures were assembled with Photoshop CS5.

Results

A Frameshift Mutation in *CHSY1* Is Identified by Homozygosity Mapping and High-Throughput Sequencing

Homozygosity mapping was performed on a Jordanian consanguineous family consisting of two unaffected parents (I:1 and I:2, Figure 1A), two affected children (II:2 and II:3, Figure 1A), and one unaffected sibling (II:1, Figure 1A). The clinical synopsis included congenital skeletal anomalies most evident on the hands and feet, symmetrical and bilateral preaxial brachydactyly, micrognathia, short stature, and variable degrees of learning disability (Figures 1B–1D; see also Figure S1). X-ray examinations revealed unified capitate and hamate bones and partial duplication of proximal phalanges of digits 1 to 3, suggestive of hyperphalangism (Figures 1C and 1D). The clinical features of the two index cases in this study match those described earlier by Dr. Samia Temtamy in another inbred family from Egypt.[11] On the basis of their comparison (Figure S1), we reason that this Jordanian family might represent another case of Temtamy Preaxial Brachydactyly Syndrome (MIM 605282).

Genotyping of the five individuals on 610k Illumina SNP arrays and subsequent identical-by-descent mapping revealed four candidate regions totaling 16.8 Mb on chromosomes 3, 5, 12, and 15 (Figure 1E). To screen the 177 candidate genes in these regions for mutations, we employed a targeted genomic loci capture[12] followed by high throughput resequencing (Figure 1F). In one affected proband, 224 genomic mismatches were identified; of these, two were homozygous and located in the coding region of *HTLF* (MIM 143089) and *CHSY1* (Table S1). The *HLTF* mutation did not cosegregate with the disease in the family. The nonsense mutation in *CHSY1*, caused by a 1 bp deletion (Figure 1F), was inherited according to the autosomal-recessive pattern inferred by this pedigree. Because *CHSY1* lies at the telomeric end of chromosome 15q, hemizygous deletions of *CHSY1* occur in patients with chromosome 15q26-qter Deletion Syndrome (MIM 612626);[13] these distinct genetic diseases share some common phenotypes, which are compared in Figure S1.

CHSY1 encodes chondroitin synthase 1, an evolutionarily conserved sugar-synthesizing enzyme present both in invertebrates and vertebrates (Figure 1G). Human CHSY1, and its paralogous protein CHSY3 (MIM 609963), consists of a carboxy-terminal type-A glycosyltransferase catalytic site and an N-terminal Fringe domain.[14,15] When aligned to the three canonical FRINGE proteins, i.e., LUNATIC (MIM 602576), MANIC (MIM 602577), and RADICAL (MIM 602578) FRINGE, the CHSY1 and CHSY3 proteins show conservation of the DXD motif, which is required for the glycosyltransferase activity of FRINGE enzymes (Figure 1H).[16,17]

The *CHSY1* Frameshift Mutation Abolishes CHSY1 Protein Synthesis and Depletes Chondroitin Sulfates in Patients

The biallelic one-base cytosine deletion in codon 32 of the ORF of *CHSY1* (c.96 del) introduces a frameshift leading to a premature stop codon 2 amino acids downstream at position 34 (p.Glu33SerFSX1). This nonsense mutation is predicted to yield a severely truncated CHSY1 protein missing both its catalytic domains (Figure 2A). To confirm the absence of CHSY1 in affected individuals, we isolated and cultured dermal fibroblasts from the male proband (II:2) and his noncarrier unaffected sibling (II:1). CHSY1, of the expected molecular weight, i.e, 88 kDa, was detected by immunoblotting in nonreducing conditions in the supernatant of primary fibroblasts but was undetectable in that of mutant fibroblasts (Figure 2B). In reducing conditions, CHSY1 migrated at 60 kDa, suggesting that the mature secreted protein might comprise two or more peptides linked by disulfide bridges. It is noteworthy that soluble CHSY1 was found to accumulate in the supernatant of primary human fibroblast cultures, whereas its primary amino acid sequence does not target it a priori for secretion. In support of our finding, CHSY1 was previously reported to be the most prominent extracellular protein in the conditioned medium of co-cultures involving myeloma cells and osteoclasts;[18] hence, CHSY1 might be processed for secretion in the Golgi via shedding of its N-terminal transmembrane domain (Figure 2A). This is in contrast to canonical FRINGE enzymes, which are known to reside in the *cis*-Golgi and not in the extracellular milieu unless overexpressed.[16]

CHSY1 is pivotal to the biosynthesis of chondroitin sulfates (CSs), which belong to the glycosaminoglycans (GAGs), consisting of alternating glucuronic acid (GlcUA) and N-acetyl galactosamine (GalNAc) residues. Once synthesized, CSs are covalently bound to side chains of extracellular proteoglycans. CHSY1 possesses both the glucuronyltransferase II and N-acetylgalactosaminyl-transferase II enzymatic activities necessary for the synthesis of the repeating disaccharide unit of CS.[14] To determine the impact of the loss of CHSY1 activity on the deposition and distribution of CSs, immunohistochemistry on patients' skin sections was performed with a monoclonal antibody directed at CS groups. Lower levels of CS in the stratum corneum, stratum germinativum, and dermal layers of the affected patient (II:2) relative to the control (II:1) were seen (Figures 2C and 2D). CS levels were also reduced in cultures of CHSY1-deficient primary fibroblasts (data not shown), which had a slower growth rate and different cell morphology than control fibroblasts (Figures 2C and 2D, insets). Taken together, our data suggest the CHSY1 is a secreted enzyme involved in the synthesis of

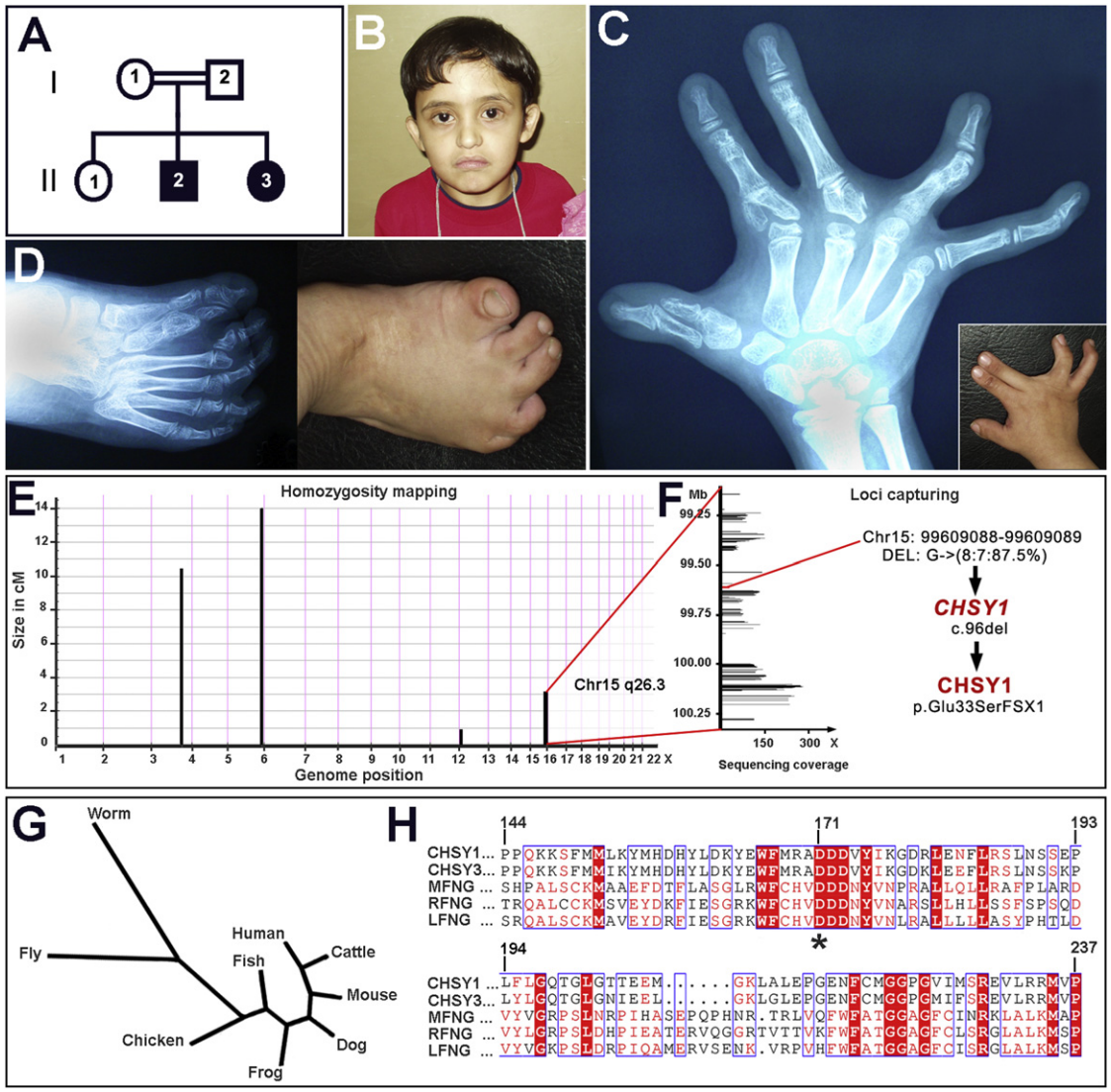

Figure 1. Phenotypic Characteristics of Investigated Patients with Syndromic Recessive Brachydactyly Caused by a Frameshift Mutation in *CHSY1*

(A) Affected children, male (II:2) and female (II:3), were born to first-cousin parents (I:1 and I:2) with one unaffected child (II:1).
(B) Head shot of affected boy (II:2) with protruding eyes, downward turn of mouth, and micrognathia.
(C) X-ray radiograph of male proband's right hand when he was 8 years of age, showing partial duplications of proximal phalanges in digits 1, 2, and 3 (inset: hand photograph).
(D) X-ray radiograph and picture of male proband's right foot showing severe skeletal anomalies. The big toe exhibits short and duplicated metatarsals and proximal phalanges. The second and fourth proximal phalanges are duplicated as well.
(E) Homozygosity mapping delineated four candidate loci totaling 19 cM on chromosomes 3, 5, 12, and 15.
(F) Genomic capturing and resequencing of candidate loci revealed a 1 bp deletion in *CHSY1* on chromosome 15; this deletion caused an early-termination stop codon at amino acid 34 of the CHSY1 enzyme.
(G) Phylogenetic tree showing conservation of CHSY1 across invertebrate and vertebrate species.
(H) The CHSY1 enzyme and its paralogous protein CHSY3 bear a Fringe domain that aligns to that of canonical MANICAL (MFNG), RADICAL (RFNG), and LUNATIC (LFNG) FRINGE. A conserved DDD motif is highlighted with a star.

CS moieties and that the reported nonsense mutation leads to a loss of function in humans.

Loss of CHSY1 Activity Triggers Massive NOTCH Activation in Patients' Cells

To gain insights into the pathogenesis of the disease, we sought to determine how secreted CHSY1 activity was coupled to known extracellular proteins causing brachydactyly in mice and humans.[1,19] Out of 16 genes whose mutations result in brachydactyly,[1,19] *CHSY1* transcripts were most correlated with those of the *NOTCH2* (MIM 600275) and *NOTCH1* (MIM 190198) receptors (Table S2). Because CHSY1 bears a Fringe domain, which modulates ligand interaction with NOTCH receptors,[20] and because NOTCH2 activation was shown to be regulated by CHSY1 levels in co-cultures of myeloma cells and osteoclasts,[18] we assessed components of the NOTCH signaling pathway in patients' primary fibroblast cell

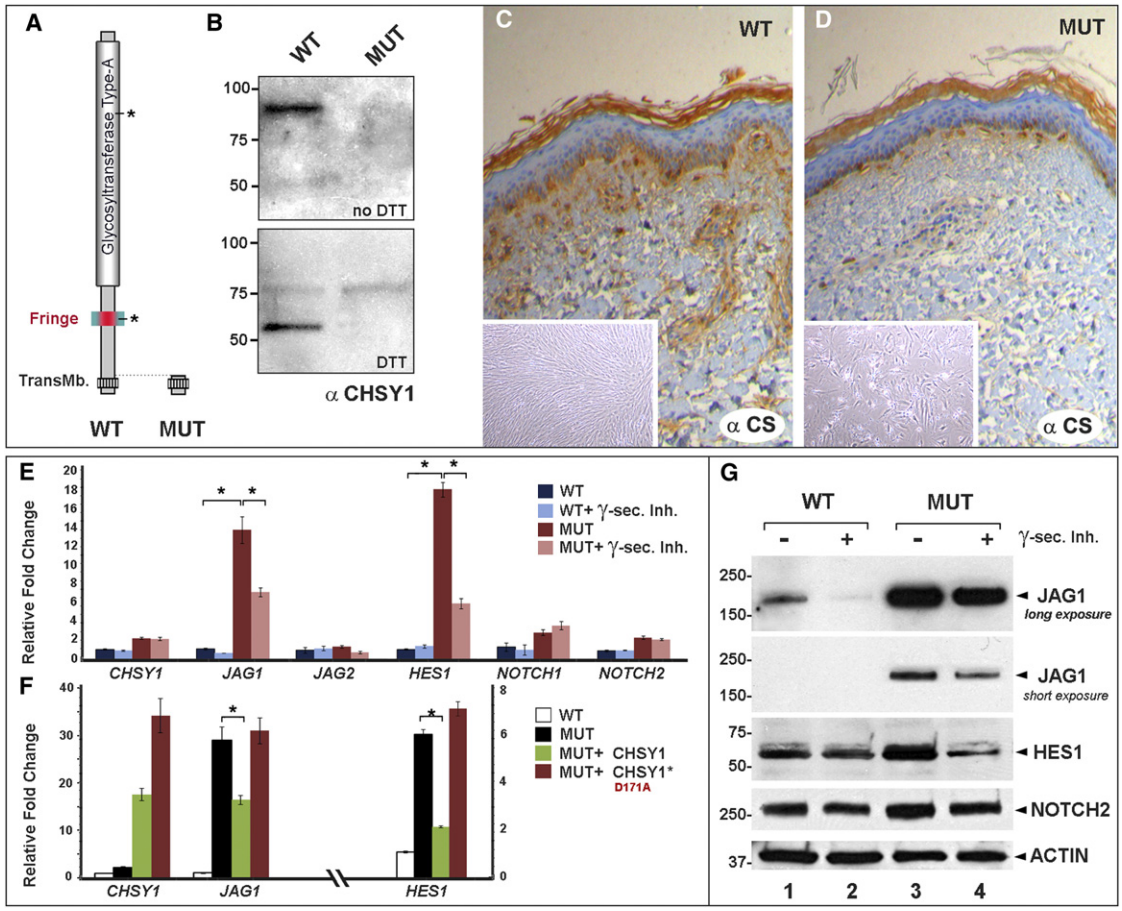

Figure 2. Loss of CHSY1 Results in Depletion of Chondroitin Sulfates and Activation of NOTCH Signaling

(A) The full-length CHSY1 (WT) consists of a type II transmembrane domain, a Fringe motif, and a type A glycosyltransferase domain. The frameshift mutation (MUT) deletes more than 95% of CHSY1, including both of its putative catalytic sites, marked with an asterisk.

(B) CHSY1 is found in the supernatant of primary fibroblast cultures from unaffected sibling II:1 (WT) but not from that of the affected proband II:2 (MUT).

(C and D) Depletion of CS, a product of the CHSY1 enzyme, is observed by immunohistochemistry in the skin of affected II:2 (D) versus unaffected sibling II:1 (C). CHSY1-deficient primary fibroblasts (D, inset) have aberrant morphologies and slower growth rates than control fibroblasts (C, inset).

(E) Massive upregulation of *JAG1* and *HES1* in affected primary fibroblasts, indicative of abnormally high NOTCH signaling, is observed by q-PCR analysis. Mutant *CHSY1* transcripts were not subjected to nonsense-mediated decay. Upregulation of NOTCH signaling was reversed by the addition of a γ-secretase inhibitor.

(F) Overexpression of intact *CHSYI*, but not of a Fringe-dead *CHSY1* D171A mutant, can reverse NOTCH activation in CHSY1-deficient fibroblasts.

(G) Abnormally high JAG1 protein production is seen in CHSY1-deficient fibroblasts (lanes 3 and 4) compared to control fibroblasts (lanes 1 and 2). Addition of a γ-secretase inhibitor rescues NOTCH activation measured by HES1 levels in CHSY1-deficient cells (compare lanes 3 and 4).

Values in (E) and (F) represent means ± SE of data from three independent experiments, *$p < 0.05$.

cultures. By quantitative PCR, relative transcript abundance of *JAG1* (MIM 601920), a NOTCH ligand, and *HES1* (MIM 139605), an immediate target of NOTCH, were found to be significantly upregulated—14-fold and 18-fold, respectively—in comparison to unaffected cells (Figure 2E). Levels of *NOTCH1* and *NOTCH2* were moderately increased. Endogenous *CHSY1* transcripts were found to be higher in *CHSY1* null cells, suggesting that the reported frameshift does not trigger the surveillance nonsense-mediated-decay pathway. Addition of a γ-secretase inhibitor, blocking NOTCH signaling at the receptor level,[21] partially rescued NOTCH over-activation in CHSY1-deficient patient cells (Figure 2E). The remarkable transcriptional upregulation of *JAG1* and *HES1* was confirmed at the protein level by immunoblotting (Figure 2G); an average 10-fold increase in JAG1 protein synthesis was seen in primary CHSY1-deficient fibroblasts at various passages (compare lanes 1 and 3, Figure 2G). Likewise, inhibiting γ-secretase activity partially rescued HES1 levels in CHSY1-deficient cells. JAG1 levels were also reduced, albeit to a lesser extent (compare lanes 3 and 4, Figure 2G).

Next, to determine whether CHSY1-mediated NOTCH inhibition required the Fringe domain, we carried out

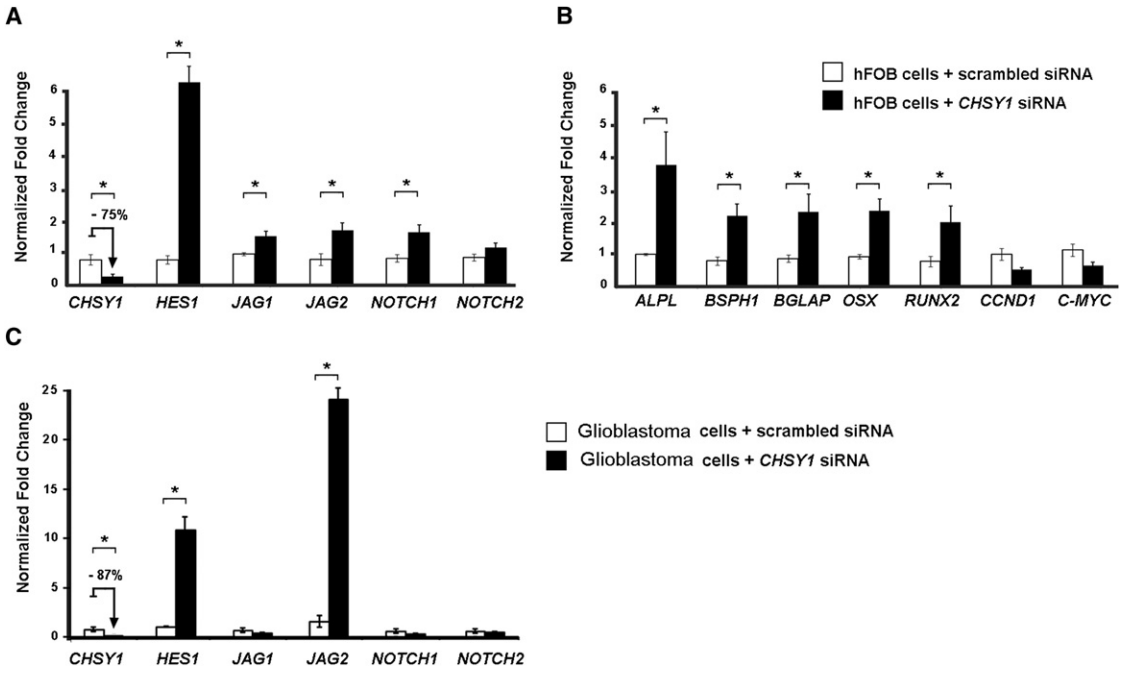

Figure 3. *CHSY1* Knockdown Promotes NOTCH Signaling and Enhances Osteogenesis In Vitro
(A) *CHSY1* siRNA in human fetal osteoblasts (hFOB) cells achieved 75% knockdown with concurrent 6-fold upregulation of *HES1*, an immediate NOTCH target. Other genes belonging to the NOTCH pathway were moderately but significantly upregulated.
(B) *CHSY1* siRNA triggered upregulation of osteogenic markers, indicative of premature differentiation, whereas proliferation markers were downregulated.
(C) *CHSY1* siRNA in human glioblastoma cells (T98G) achieved 87% knockdown and a paralleled 10-fold upregulation of *HES1* and 24-fold increase in *JAG2* transcription.
Values in (A)–(C) represent means ± SE of data from three independent experiments, *$p < 0.05$.

rescue experiments in patients' primary cells. NOTCH upregulation in CHSY1-deficient cells could only be reversed by transfection of wild-type human *CHSY1* but not of a D171A Fringe catalytically dead mutant construct[17] (Figure 2F), indicating that CHSY1 requires an intact Fringe domain to execute its function. Together, these results argue that secreted CHSY1, via its Fringe domain, exerts NOTCH inhibitory activity in human primary skin fibroblasts and that its absence triggers massive JAG1 protein synthesis.

CHSY1 Knockdown by siRNA in Human Osteoblast Progenitor Cells Triggers NOTCH Activation and Premature Osteogenic Differentiation

To address the ossification anomalies, we then modeled loss of *CHSY1* by siRNA in a human fetal osteoblast (hFOB) progenitor cell line (Figures 3A and 3B). *CHSY1* siRNA, which achieved more than 75% knockdown efficiency, resulted in markedly increased NOTCH signaling, as indicated by the 6-fold increase in the abundance of *HES1* transcripts (Figure 3A); levels of *JAG1*, *JAG2* (MIM 602570), and *NOTCH1* were moderately but significantly increased. Concurrent with NOTCH upregulation, markers of osteogenic differentiation such as *ALPL* (MIM 171760), *BSPH1* (MIM 147563), *BGLAP* (MIM 112260), *OSX* (MIM 606633), and *RUNX2* (MIM 600211) were significantly augmented, whereas markers of proliferation such as *CCND1* (MIM 168461) and *C-MYC* (MIM 190080) were reduced (Figure 3B). Alkaline phosphatase activity was increased by 40% (data not shown). Taken together, these results suggest that *CHSY1* knockdown, which leads to NOTCH activation, suffices to bring about premature, or enhanced, osteogenic differentiation in a hFOB progenitor cell line. These in vitro data provide a possible pathomechanism for the observed accessory bones and hyperphalangism seen in the two affected children.

To substantiate CHSY1's specificity on NOTCH signaling, we repeated RNAi knockdown in a human neural glioblastoma cell line (Figure 3C). Unexpectedly, *JAG2*, but not *JAG1* as in primary patient fibroblasts, was greatly increased (24-fold). As in hFOB and patient primary cells, *HES1* levels were also upregulated, indicative of robust NOTCH activation. Together, these in vitro experiments argue that CHSY1 bears widespread repressive activity on NOTCH signaling and that this inhibition is likely to be gene and tissue specific.

Loss of Function of *chsy1* in Zebrafish Embryos Impairs Skeletogenesis and Leads to Increased Notch Signaling

To model, in vivo, the birth defects observed in *CHSY1* mutant individuals, we next performed *chsy1* morpholino (MO) injections in developing zebrafish embryos (Figure 4). To block translation of maternal and zygotic *chsy1*

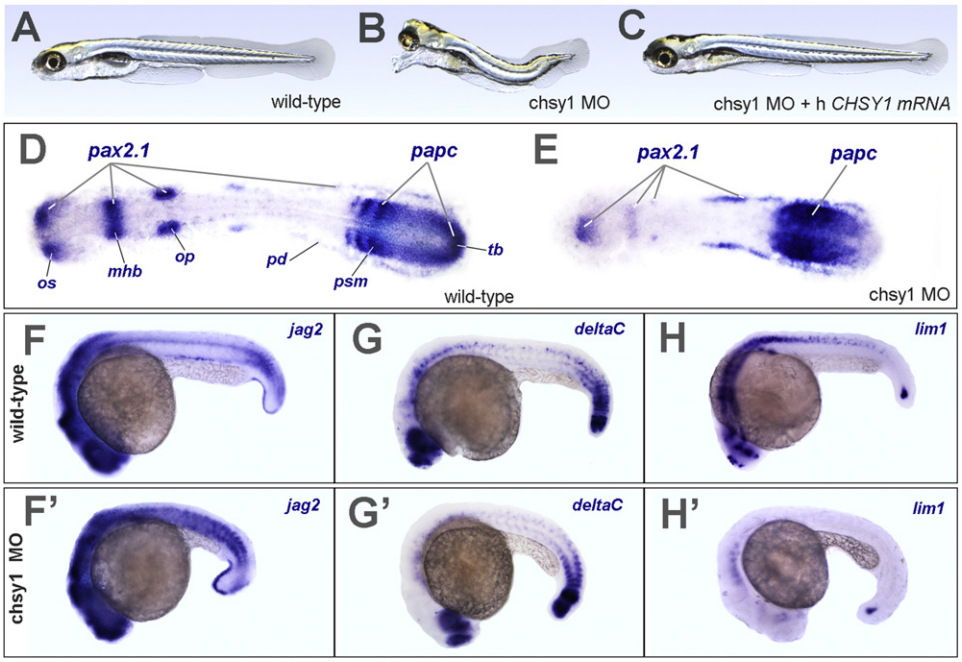

Figure 4. *chsy1* Knockdown in Zebrafish Embryos Affects Segmentation and Increases Notch Signaling
(A) Six-day-old wild-type embryo.
(B) Six-day-old *chsy1* MO-injected embryo with a protruding mouth-piece, eyes joined at the midline, and arched trunk.
(C) Six-day-old *chsy1* MO-injected embryo rescued with 200 pg of human *CHSY1* mRNA.
(D) Ten-somite-stage wild-type embryo stained with *pax2.1* marking the optic stalk (os), midbrain-hindbrain boundary (mhb), otic placodes (op), and pronephric duct (pd) and with *papc* marking the pre-somitic mesoderm (psm) and the tailbud (tb).
(E) Ten-somite stage *chsy1* morphant embryo displays a fused anterior eyefield, near-absent isthmic organizer, and otic placodes marked by *pax2.1*. Aberrant segmentation of the pre-somitic mesoderm and lack of *papc* staining in the tailbud indicate anomalies in somitogenesis.
(F and F′) Wild-type (F) and *chsy1* morphant (F′) 24 hpf embryos stained for the Notch ligand *jag2*. Note ectopic or delayed clearance of *jag2* expression in trunk somites.
(G and G′) Wild-type (G) and *chsy1* morphant (G′) 24 hpf embryos stained for the Notch ligand *deltaC*. Note the enhanced expression in presomitic mesoderm at the tailbud level.
(H and H′) Wild-type (H) and *chsy1* morphant (H′) 24 hpf embryos that were stained with *lim1* and whose expression is downregulated by Notch signaling. The loss of *lim1* expression in head and trunk structures indicates greater-than-normal Notch signaling in *chsy1* morphants relative to controls.

transcripts, we used two MOs against *chsy1*, as previously described.[22] *chsy1* was ubiquitously present from the unfertilized oocyte to the end of somitogenesis (Figure S2). By day two, its expression was limited to head structures; there was prominent expression in the inner ear and diffuse expression in developing chondrocytes of the pectoral-fin bud (Figure S2J). Compared to wild-type siblings at 6 days (Figure 4A), morphant *chsy1* embryos developed into stunted larvae with severe eye anomalies and cartilage and pectoral-fin defects (Figure 4B). The specificity of the MOs was addressed by rescue experiments; *chsy1* MOs were coinjected with human *CHSY1* mRNA at the one-cell stage. In 87% (n = 149/171) of the coinjected embryos, *chsy1* morphant phenotypes were rescued (Figure 4C; see also Table S3). At the ten-somite stage, *chsy1* morphants exhibited obvious segmentation anomalies marked by poorly segmented presomitic mesoderm and absence of *papc* expression in the tailbud (Figures 4D and 4E). Anterior defects in *chsy1* morphants comprised a single anterior eyefield, as opposed to split eyefields in control embryos, and reduced *pax2.1* expression in otic placodes and in the midbrain-hindbrain boundary (Figures 4D and 4E). By 24 hpf, expression of the two notch ligands *jag2* and *deltaC* was increased in *chsy1* morphants as compared to wild-type embryos (Figures 4 F–4G′), *jag2* was found to be ectopically expressed in trunk paraxial mesoderm, indicative of impaired segmentation, whereas *deltaC* levels in tailbud and presomitic mesoderm were enhanced (Figures 4F–4G′). We next assessed *lim1*, a target of Notch signaling whose expression is repressed by the Notch pathway.[23] Reflecting greater-than-normal Notch activity in *chsy1* morphants, *lim1* expression was visibly dampened in head and trunk structures relative to those of control embryos (Figures 4H and 4H′). Collectively, these results indicate that *chsy1* activity is essential for toning down Notch signaling across various embryonic structures during zebrafish development.

Zebrafish *chsy1* Morphant Embryos Partially Phenocopy Human Disorder

By day 5, zebrafish *chsy1* morphant embryos exhibited major skeletal anomalies encompassing severe jaw

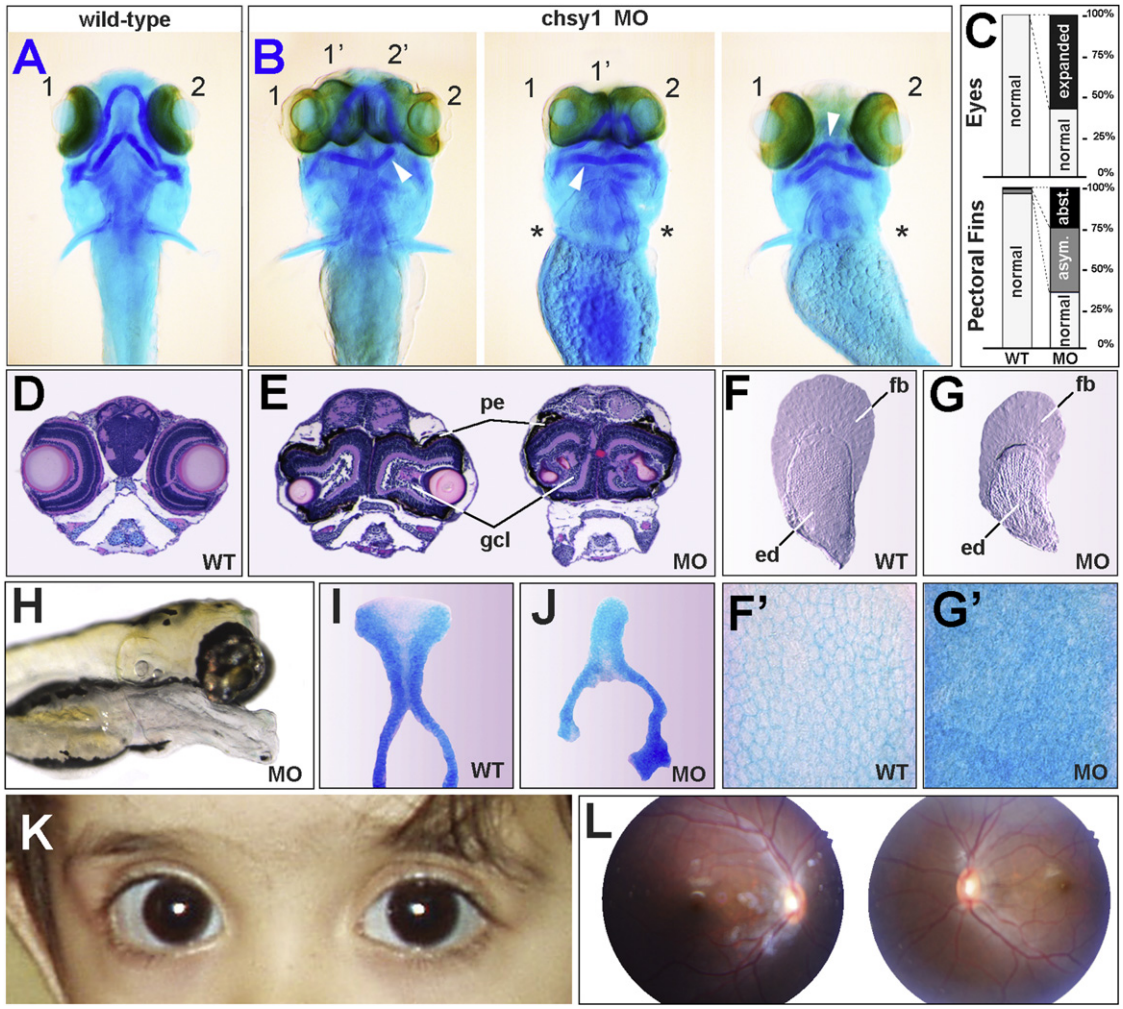

Figure 5. Phenotypes of *chsy1* Zebrafish Morphant Embryos Partially Phenocopy Human Disorder
(A) Ventral view of alcian-blue-stained 5-day-old wild-type embryo.
(B) Three representative *chsy1* MO-injected embryos exhibiting variable phenotypic penetrance, including skeletal anomalies (arrowheads), massive overgrowth of retinas, and pectoral-fin defects ranging from asymmetric development to unilateral or bilateral aplasia (asterisks).
(C) Percentage of eyes and pectoral-fin defects scored in *chsy1* MO compared to wild-type embryos. (Asym., asymmetric; Abst., absent).
(D) Hematoxylin and Eosin (H&E) head sections of 5-day-old wild-type embryo.
(E) H&E sections through midline-joining retinas of *chsy1* morphant embryos at 5 days of development. Note hyperplasia of pigmented epithelium (pe) and increased cell numbers in the ganglion cell layer (gcl).
(F and F′) Pectoral fin of a 6-day-old wild-type embryo. (F′) High-magnification view of the endoskeletal disc showing cartilage tissue with monolayered chondrocytes stained with alcian blue.
(G and G′) Pectoral fin of a mildly affected 6-day-old *chsy1* MO-injected embryo exhibiting hypoplasia of the endoskeletal disc (ed) relative to the fin blade (fb). (G′) High-magnification view of cartilage tissue with multilayered disorganized chondrocytes in the endoskeletal disc of *chsy1* morphant embryo stained with alcian blue.
(H) Lateral view of 5-day-old *chsy1* morphant embryos with severe jaw hypoplasia and eye defects.
(I) Ethmoid plate of a 5-day-old wild-type embryo stained with alcian blue.
(J) Irregularly shaped ethmoid plate of a 5-day-old *chsy1* morphant embryo.
(K) Affected girl (II:3), showing bilateral macrophthalmia and blue sclera.
(L) Color fundus photographs of affected girl (II:3) at 6 years of age. The girl had bilateral tilted eye discs and normal visual acuity in each eye.

hypoplasia, impaired pectoral-fin development, and prominent eyes (Figures 5A–5G′). The anterior paired pectoral fins, which are analogous to the mammalian forelimbs, were affected in 65% (n = 94/144) of MO-injected embryos (Figure 5C). Anomalies in the development of the pectoral fins ranged from pronounced asymmetries to unilateral or bilateral aplasia (Figures 5A and 5B). Bright-field images of dissected pectoral fins from mildly affected *chsy1*-morphant embryos revealed structural anomalies of the endoskeletal disc, a structure analogous to the bones found in higher pentadactyl vertebrates. In contrast, fin blades, of which no equivalent tissue exists in mammals, were relatively normal in morphants (Figures 5F and 5G). Higher magnification of alcian-blue-stained chondrocytes

in the *chsy1*-morphant limb buds revealed a disorganized, multilayered tissue (Figure 5G′) as opposed to the monolayer tissue organization in wild-type limb buds (Figure 5F′). Other remarkable cartilage defects, including disgenesis of the ethmoid plate (Figures 5I and 5J), in the neurocranium resulted in a protruding-snout, "seahorse" phenotype (Figure 5H).

Unexpectedly, eye anomalies were also present in more than 50% (n = 84/144) of morphant embryos (Figures 5A–5E). In extreme cases, *chsy1* morphants developed four eyes resembling complete bilateral retinal duplications (Figure 5B). Histological examination showed instead one pair of overgrown retinas, which joined at the midline. No lens duplication was recorded. *chsy1* morphant eyes presented with the expected retinal cell layers but had augmented cell numbers in the ganglion cell layer and the pigmented epithelium (Figures 5D and 5E). This prominent eye phenotype found in *chsy1* morphant fish prompted us to re-examine our two human index cases for possible ocular anomalies. Fundoscopic evaluations did not reveal altered retinal thickness, but we noted that both probands exhibited macrophthalmia accompanied by bilateral blue sclera, remnants of pupillary membrane over the crystalline lens, and tilted optic discs in both eyes (Figures 5K and 5L). This suggests that *CHSY1* may play a role in eye morphogenesis in humans as well. Thus, knockdown of *chsy1* in zebrafish embryos revealed a conserved role for CHSY1 during embryogenesis in vertebrates. The phenotypes observed upon knockdown of *chsy1* in fish partially phenocopy the human disorder, revealing a conserved role for CHSY1 in skeletal development and limb morphogenesis during vertebrate embryogenesis.

Discussion

In summary, loss of CHSY1 is a cause of recessive syndromic brachydactyly and evokes phenotypes that overlap with mutations in the BMP, GDF, and Hedgehog pathways.[1] The pathophysiological basis of this syndrome appears to be enhanced, or premature, ossification—possibly driven by greater-than-normal NOTCH signaling—leading to congenital skeletal anomalies most obvious in digits. This is consistent with studies performed in mice, where appropriate Notch signaling was found to be essential for the normal progression of chondrocyte differentiation into bone in the developing appendicular and axial skeletal elements.[24] The particular splitting of proximal phalanges in digits 1, 2, and 3 in this syndrome might be explained by double epiphyses growing along the longitudinal, rather than horizontal, axis. An analogous situation has been reported in Brachydactyly type A2, caused by mutations in *GDF5*, where a single epiphysis, albeit turned, results in a triangular bone.[3]

At the molecular level, we propose that CHSY1 inhibits the NOTCH pathway in the extracellular space via its Fringe domain. The aberrant production of JAG1 protein in human CHSY1-deficient fibroblasts raises the possibility that ectopic NOTCH signaling mediated by JAG1 during embryogenesis could in part be responsible for the birth defects specific to this syndrome. Control of CHSY1 activity in a tissue-specific manner may therefore constitute a therapeutic target for patients with Alagille syndrome (MIM 118450) caused by JAG1 haploinsufficiency.[25,26]

We speculate that CHSY1, which needs an intact Fringe domain to exert its NOTCH inhibitory activity, might post-translationally modify NOTCH-related proteins. However, substantiating that NOTCH receptors, or their ligands, are actual substrates of CHSY1 will require biochemical evidence. If so, CSs, of which two paralogs exist in the human genome, might function as a new class of FRINGE enzymes controlling NOTCH output during developmental, physiological, or pathological processes. Concurrently and alternatively, CHSY1 loss, which leads to reduced CS moieties and therefore altered proteoglycan synthesis, might affect other signaling pathways associated with brachydactylies. When one considers that sulfated glycans can modulate FGF/FGFR interactions, that CS affect IHH signaling,[27,28] and that both FGF and IHH can in turn regulate BMP/GDF,[29] it is conceivable that reduced CS might impede digit development by altering these pathways, instead of or in addition to NOTCH signaling.

The in vivo knock-down experiments carried out in zebrafish embryos confirmed *chsy1*'s role during skeletogenesis and unmasked its importance during eye development. Emulating the results obtained in cell culture, Notch over-activation, marked by *jag2* upregulation and silencing of *lim1*, in *chsy1* morphant embryos argues that *chsy1* is also necessary for driving repression of Notch signaling during development. It is noteworthy that *chsy1* morphant embryos bear striking resemblance to the maternal zebrafish mutant *pug* described by the group of Mary Mullins.[30] *Pug* mutants lack pectoral fins, have eyes joined at the midline, and present with segmentation anomalies similar to what is described here. It is therefore tempting to speculate that *pug* might be a *chsy1* maternal mutant. Although *chsy1* and *pug* might not be allelic, these two genes might instead delineate a common pathway controlling limb patterning in addition to the oocyte-to-embryo transition. In support of CHSY1's putative role in the earliest stages of development, RNA-interference-mediated depletion of *ChSy* (paralogous to human *CHSY1*) in *C. elegans* triggers cytokenesis reversal, and blocks cell divisions at the 2- to 4-cell stage.[31] Should CHSY1's role during oogenesis be conserved in humans, we are aware that the reported loss-of-function mutation in this study would only unmask the zygotic function of *CHSY1*. In contrast, a biallelic maternal mutation might lead to early embryonic lethality, and signs of sterility in homozygous *CHSY1* mutant women should hereafter be anticipated.

Supporting Data

In the same issue, Li et al. report on the characterization of five loss-of-function alleles of *CHSY1* as being responsible

for Temtamy Preaxial Brachydactyly Syndrome. With the exception of hearing loss, clinical manifestations in their affected cases match those described in the two proband herein. Their work indicates that transcriptional regulation of *chsy1* expression in zebrafish is regulated by the BMP pathway, which is a prominent cause of brachydactylies in humans. Taken together, our findings outline a possible means, through CHSY1 regulation, by which BMP signals are coupled to NOTCH signaling, a scenario often reiterated during the course of discreet developmental programs.

Supplemental Data

Supplemental Data include two figures and four tables and can be found with this article at http://www.cell.com/AJHG/.

Acknowledgments

We are indebted to the family for kindly partaking in this study. We thank H. Hall, K. Rogers, and S. Rogers for their diligent expertise with histology. The help of C.Y. Lim, C. Bonnard, N. Beillard, L. Ho, and S. Chng is gratefully acknowledged. We are also grateful to K. Sampath, Y-J. Jiang, and K. Sugahara for sharing reagents and to S. Roy for teaching us how to dissect pectoral fins. This study was supported by grants from A*STAR and the Society in Science Branco Weiss Foundation to B.R.

Received: September 16, 2010
Revised: November 3, 2010
Accepted: November 12, 2010
Published online: December 2, 2010

Web Resources

The URLs for data presented herein are as follows:

Blat-like Fast Accurate Search Tool (BFAST)[32], http://sourceforge.net/apps/mediawiki/bfast/index.php?title=Main_Page
Ensembl, http://www.ensembl.org
HapMap Phase II recombination rate map, http://www.hapmap.org/downloads/recombination/latest/
Human reference genome (UCSC build 18), http://genome.ucsc.edu
GenBank, http://www.ncbi.nlm.nih.gov/mapview
Gene-gene correlation tool[33], http://genome.ucla.edu/~jdong/GeneCorr.html
Online Mendelian Inheritance in Man (OMIM), http://www.ncbi.nlm.nih.gov/omim
Pipeline for sequence analysis (SeqWare Pipeline), http://seqware.sourceforge.net
Reversade laboratory's website, http://www.reversade.com

References

1. Temtamy, S.A., and Aglan, M.S. (2008). Brachydactyly. Orphanet J. Rare Dis. *3*, 15.
2. Lehmann, K., Seemann, P., Silan, F., Goecke, T.O., Irgang, S., Kjaer, K.W., Kjaergaard, S., Mahoney, M.J., Morlot, S., Reissner, C., et al. (2007). A new subtype of brachydactyly type B caused by point mutations in the bone morphogenetic protein antagonist NOGGIN. Am. J. Hum. Genet. *81*, 388–396.
3. Seemann, P., Schwappacher, R., Kjaer, K.W., Krakow, D., Lehmann, K., Dawson, K., Stricker, S., Pohl, J., Plöger, F., Staub, E., et al. (2005). Activating and deactivating mutations in the receptor interaction site of GDF5 cause symphalangism or brachydactyly type A2. J. Clin. Invest. *115*, 2373–2381.
4. Dathe, K., Kjaer, K.W., Brehm, A., Meinecke, P., Nürnberg, P., Neto, J.C., Brunoni, D., Tommerup, N., Ott, C.E., Klopocki, E., et al. (2009). Duplications involving a conserved regulatory element downstream of BMP2 are associated with brachydactyly type A2. Am. J. Hum. Genet. *84*, 483–492.
5. Lehmann, K., Seemann, P., Stricker, S., Sammar, M., Meyer, B., Süring, K., Majewski, F., Tinschert, S., Grzeschik, K.H., Müller, D., et al. (2003). Mutations in bone morphogenetic protein receptor 1B cause brachydactyly type A2. Proc. Natl. Acad. Sci. USA *100*, 12277–12282.
6. Schwabe, G.C., Tinschert, S., Buschow, C., Meinecke, P., Wolff, G., Gillessen-Kaesbach, G., Oldridge, M., Wilkie, A.O., Kömec, R., and Mundlos, S. (2000). Distinct mutations in the receptor tyrosine kinase gene ROR2 cause brachydactyly type B. Am. J. Hum. Genet. *67*, 822–831.
7. Gao, B., Guo, J., She, C., Shu, A., Yang, M., Tan, Z., Yang, X., Guo, S., Feng, G., and He, L. (2001). Mutations in IHH, encoding Indian hedgehog, cause brachydactyly type A-1. Nat. Genet. *28*, 386–388.
8. Sun, M., Ma, F., Zeng, X., Liu, Q., Zhao, X.L., Wu, F.X., Wu, G.P., Zhang, Z.F., Gu, B., Zhao, Y.F., et al. (2008). Triphalangeal thumb-polysyndactyly syndrome and syndactyly type IV are caused by genomic duplications involving the long range, limb-specific SHH enhancer. J. Med. Genet. *45*, 589–595.
9. Klopocki, E., Hennig, B.P., Dathe, K., Koll, R., de Ravel, T., Baten, E., Blom, E., Gillerot, Y., Weigel, J.F., Krüger, G., et al. (2010). Deletion and point mutations of PTHLH cause brachydactyly type E. Am. J. Hum. Genet. *86*, 434–439.
10. Johnson, D., Kan, S.H., Oldridge, M., Trembath, R.C., Roche, P., Esnouf, R.M., Giele, H., and Wilkie, A.O. (2003). Missense mutations in the homeodomain of HOXD13 are associated with brachydactyly types D and E. Am. J. Hum. Genet. *72*, 984–997.
11. Temtamy, S.A., Meguid, N.A., Ismail, S.I., and Ramzy, M.I. (1998). A new multiple congenital anomaly, mental retardation syndrome with preaxial brachydactyly, hyperphalangism, deafness and orodental anomalies. Clin. Dysmorphol. *7*, 249–255.
12. Lee, H., O'Connor, B.D., Merriman, B., Funari, V.A., Homer, N., Chen, Z., Cohn, D.H., and Nelson, S.F. (2009). Improving the efficiency of genomic loci capture using oligonucleotide arrays for high throughput resequencing. BMC Genomics *10*, 646.
13. Rump, P., Dijkhuizen, T., Sikkema-Raddatz, B., Lemmink, H.H., Vos, Y.J., Verheij, J.B., and van Ravenswaaij, C.M. (2008). Drayer's syndrome of mental retardation, microcephaly, short stature and absent phalanges is caused by a recurrent deletion of chromosome 15(q26.2—>qter). Clin. Genet. *74*, 455–462.
14. Kitagawa, H., Uyama, T., and Sugahara, K. (2001). Molecular cloning and expression of a human chondroitin synthase. J. Biol. Chem. *276*, 38721–38726.
15. Yada, T., Sato, T., Kaseyama, H., Gotoh, M., Iwasaki, H., Kikuchi, N., Kwon, Y.D., Togayachi, A., Kudo, T., Watanabe, H., et al. (2003). Chondroitin sulfate synthase-3. Molecular cloning and characterization. J. Biol. Chem. *278*, 39711–39725.

16. Johnston, S.H., Rauskolb, C., Wilson, R., Prabhakaran, B., Irvine, K.D., and Vogt, T.F. (1997). A family of mammalian Fringe genes implicated in boundary determination and the Notch pathway. Development *124*, 2245–2254.
17. Munro, S., and Freeman, M. (2000). The notch signalling regulator fringe acts in the Golgi apparatus and requires the glycosyltransferase signature motif DXD. Curr. Biol. *10*, 813–820.
18. Yin, L. (2005). Chondroitin synthase 1 is a key molecule in myeloma cell-osteoclast interactions. J. Biol. Chem. *280*, 15666–15672.
19. Pan, Y., Liu, Z., Shen, J., and Kopan, R. (2005). Notch1 and 2 cooperate in limb ectoderm to receive an early Jagged2 signal regulating interdigital apoptosis. Dev. Biol. *286*, 472–482.
20. Hicks, C., Johnston, S.H., diSibio, G., Collazo, A., Vogt, T.F., and Weinmaster, G. (2000). Fringe differentially modulates Jagged1 and Delta1 signalling through Notch1 and Notch2. Nat. Cell Biol. *2*, 515–520.
21. Milano, J., McKay, J., Dagenais, C., Foster-Brown, L., Pognan, F., Gadient, R., Jacobs, R.T., Zacco, A., Greenberg, B., and Ciaccio, P.J. (2004). Modulation of notch processing by gamma-secretase inhibitors causes intestinal goblet cell metaplasia and induction of genes known to specify gut secretory lineage differentiation. Toxicol. Sci. *82*, 341–358.
22. Zhang, J., Lefebvre, J.L., Zhao, S., and Granato, M. (2004). Zebrafish unplugged reveals a role for muscle-specific kinase homologs in axonal pathway choice. Nat. Neurosci. *7*, 1303–1309.
23. Appel, B., Givan, L.A., and Eisen, J.S. (2001). Delta-Notch signaling and lateral inhibition in zebrafish spinal cord development. BMC Dev. Biol. *1*, 13.
24. Mead, T.J., and Yutzey, K.E. (2009). Notch pathway regulation of chondrocyte differentiation and proliferation during appendicular and axial skeleton development. Proc. Natl. Acad. Sci. USA *106*, 14420–14425.
25. Li, L., Krantz, I.D., Deng, Y., Genin, A., Banta, A.B., Collins, C.C., Qi, M., Trask, B.J., Kuo, W.L., Cochran, J., et al. (1997). Alagille syndrome is caused by mutations in human Jagged1, which encodes a ligand for Notch1. Nat. Genet. *16*, 243–251.
26. Boyer-Di Ponio, J., Wright-Crosnier, C., Groyer-Picard, M.T., Driancourt, C., Beau, I., Hadchouel, M., and Meunier-Rotival, M. (2007). Biological function of mutant forms of JAGGED1 proteins in Alagille syndrome: inhibitory effect on Notch signaling. Hum. Mol. Genet. *16*, 2683–2692.
27. Cortes, M., Baria, A.T., and Schwartz, N.B. (2009). Sulfation of chondroitin sulfate proteoglycans is necessary for proper Indian hedgehog signaling in the developing growth plate. Development *136*, 1697–1706.
28. Häcker, U., Nybakken, K., and Perrimon, N. (2005). Heparan sulphate proteoglycans: The sweet side of development. Nat. Rev. Mol. Cell Biol. *6*, 530–541.
29. Minina, E., Kreschel, C., Naski, M.C., Ornitz, D.M., and Vortkamp, A. (2002). Interaction of FGF, Ihh/Pthlh, and BMP signaling integrates chondrocyte proliferation and hypertrophic differentiation. Dev. Cell *3*, 439–449.
30. Wagner, D.S., Dosch, R., Mintzer, K.A., Wiemelt, A.P., and Mullins, M.C. (2004). Maternal control of development at the midblastula transition and beyond: Mutants from the zebrafish II. Dev. Cell *6*, 781–790.
31. Mizuguchi, S., Uyama, T., Kitagawa, H., Nomura, K.H., Dejima, K., Gengyo-Ando, K., Mitani, S., Sugahara, K., and Nomura, K. (2003). Chondroitin proteoglycans are involved in cell division of Caenorhabditis elegans. Nature *423*, 443–448.
32. Homer, N., Merriman, B., and Nelson, S.F. (2009). BFAST: An Alignment Tool for Large Scale Genome Resequencing. PLoS ONE *4*, e7767.
33. Day, A., Dong, J., Funari, V.A., Harry, B., Strom, S.P., et al. (2009). Disease gene characterization through large-scale co-expression analysis. PLoS ONE *4*, e8491.